

# **CONTROL OF LARGE COMMUNICATION SATELLITES**

**Richard Gran**

**Michael Proise**

**Alex Zislin**

**Grumman Aerospace Corporation**

**Bethpage, New York 11714**

## **ABSTRACT**

Control of large communication satellites becomes most difficult when the structure gets large enough that the structural motion severely impacts the ability to stabilize the RF antennas. This structural/control interaction means that the control engineer can no longer use “benign neglect” of the structural vibrations, but must design a control that has a bandwidth that exceeds the lowest structural vibratory frequency. This in itself is not a problem as long as the sensors and actuators are colocated. Eventually, the antennas have to be controlled independently and the assumption of colocated sensors and actuators is no longer reasonable. This begins the problem. In this paper, the various approaches that have been proposed for controlling large flexible spacecraft when the structural frequencies and the control frequencies overlap will be described. A new approach to the design of such systems will be described, and a reasonably complex example of a large satellite control will be described. The presentation will show a movie that was produced to illustrate the control of this structure and the consequence of using the approach described in the paper.

## **INTRODUCTION**

The communication satellite (comsat) control problem is unique. The specification for these controllers simply demands accurate steady state performance in the presence of random perturbations. No settling time, overshoot or other transient performance criteria are imposed on the controller. Solar induced torques, gravity gradient torques, geomagnetic torques are the environmental disturbances on the satellite that cause the attitude to be perturbed. The sensors have their own inherent noise plus they pick up internal vibration noises on the satellite. The effect of these noises is to torque the satellite in a random way that depends upon the control gains and the type of actuator that is used. All of these disturbances may be very accurately modeled using stochastic modeling techniques. The result is a set of dynamic models that consist of linear systems excited by white noises that can be used to design a control system that has the best possible

response. This “best” response may be achieved by minimizing the uncertainty in the attitude and rate of the rigid body of the spacecraft.

The procedure for determining the best gains is to compute the covariance matrix for the dynamic model of the spacecraft excited by all of the noises that are expected. This covariance will depend on the gains in the control system feedback loops (which are to be determined). The appropriate variances are then minimized to determine the best gains.

The control problem then follows the steps:

- Characterize the dynamics of the satellite by developing linear models of
  - Rigid body
  - Momentum exchange devices (or other controller dynamics)
  - Gravity gradient effect on rigid body
  - Flexible appendage dynamics
- Specify and characterize the disturbance torques
  - Solar torques (due to solar array and these are at orbital period)
  - High frequency solar effect due to variations in solar wind etc.
  - Electromagnetic torques created by the interaction of the earth’s field and magnetic torques created on the spacecraft. In the designs discussed here, these torques are deliberately created to provide magnetic control.
  - Reaction jet torques created by the thrust uncertainty and c.g. uncertainty
  - Sensor noises characterized by the power spectral density functions (PSD’s)
- Specify the control configuration, i.e. what will be measured, what gains will be used, and what actuators will be employed. Generally “full state” feedback will be used to provide that control with the best gain and phase margin.
- Find the values of the gains that minimizes the variances of the appropriate dynamic states (attitude or rate).
- Verify the design using the structural dynamics model for appendage and spacecraft vibration modes

Notice that this design procedure does not yield a design that has been dubbed a “modern modal controller” in that the resulting control system simply consists of a set of gains that were selected for the best noise response. This structure is very simple and easy to implement. The modern modal controller on the other hand assumes that the measurements are processed through an optimal filter (a Kalman filter) which determines a best estimate of the spacecraft attitude, rate and other dynamic states. It is the estimated states that are then used for controller feedback. This design has many disadvantages. It is very sensitive to the assumed dynamic model (particularly when the model contains the flexible motion). The design is usually such that the gain and phase margins are poor. The designs require a model of the spacecraft dynamics be built in the computer (for the filter) so the design is more complex and difficult to implement.

The design approach we have outlined above is described in the following section, and a typical spacecraft design that illustrates this approach is described in the last section.

## OPTIMAL FULL STATE STOCHASTIC CONTROL FOR COMSAT APPLICATIONS

Consider the stochastic system defined by

$$\begin{aligned}\dot{\underline{x}} &= A \underline{x} + B \underline{u} + c \underline{w} \\ \underline{y} &= M \underline{x} + \underline{v}\end{aligned}\tag{1}$$

where:  $\underline{x}$  is the system state vector of dimension  $n$   
 $\underline{y}$  is the noisy full state measurement of  $\underline{x}$  (i.e.  $M$  is nonsingular)  
 $\underline{w}$  is a unit variance white noise excitation that is independent of  $\underline{v}$   
 $\underline{v}$  is the  $n$  dimensional white measurement noise with  $E(\underline{v} \underline{v}^T) = R \delta(t)$   
 $\underline{u}$  is the control  
 $A, B,$  and  $C$  are the state, control and noise influence matrices respectively

The covariance matrix  $P = \{(\underline{x} - E(\underline{x}))(\underline{x} - E(\underline{x}))^T\}$  satisfies a differential equation

$$\dot{P} = A P + P A^T + C C^T\tag{2}$$

if the control  $\underline{u}$  is not random. If the control system is assumed to be linear, then the control  $\underline{u}$  is given by

$$\underline{u} = K \underline{y} = K (M \underline{x} + \underline{v}).\tag{3}$$

The control in (3) is clearly random because of the measurement noise  $\underline{v}$ . Thus (2) is no longer the covariance matrix equation. The correct equation is obtained by substituting (3) into (1). Thus we get

$$\dot{P} = (A + BKM) P + P (A+BKM)^T + BK R K^T B^T + C C^T\tag{4}$$

If equation (4) is written in such a way that the quadratic in  $K$  is made explicit on the right hand side, the result is

$$\begin{aligned}P (B K + P M^T R^{-1} R (B K + P M^T R^{-1})^T \\ + A P + P A^T + C C^T - P M^T R^{-1} M P).\end{aligned}\tag{5}$$

To determine the gain that minimizes any linear combination of components of  $P$  is now easy since the quadratic term in  $K$  that appears on the right hand side of (5) is always

greater than or equal to zero (since R is always positive definite). Thus the smallest that  $\dot{P}$  can be is when the quadratic is zero ( $\dot{P}$  small or equivalently the smallest P in steady state when  $\dot{P}$  is zero). Hence the optimal minimizing gain is given by

$$B K = - P M^T R^{-1} \text{ or } K = - (B^T B)^{-1} B^T P M^T R^{-1} \quad (6)$$

and the covariance matrix P is the solution of the Riccati equation

$$\dot{P} = A P + P A^T + C C^T - P M^T R^{-1} M F \quad (7)$$

It is obvious that this solution is not what one would get were one optimizing a performance measure of the form

$$J = E \left\{ \int_{t_0}^{t^*} ( \underline{x}^T \tilde{Q} \underline{x} + \underline{u}^T \tilde{R} \underline{u} ) dt \right\} \quad (8)$$

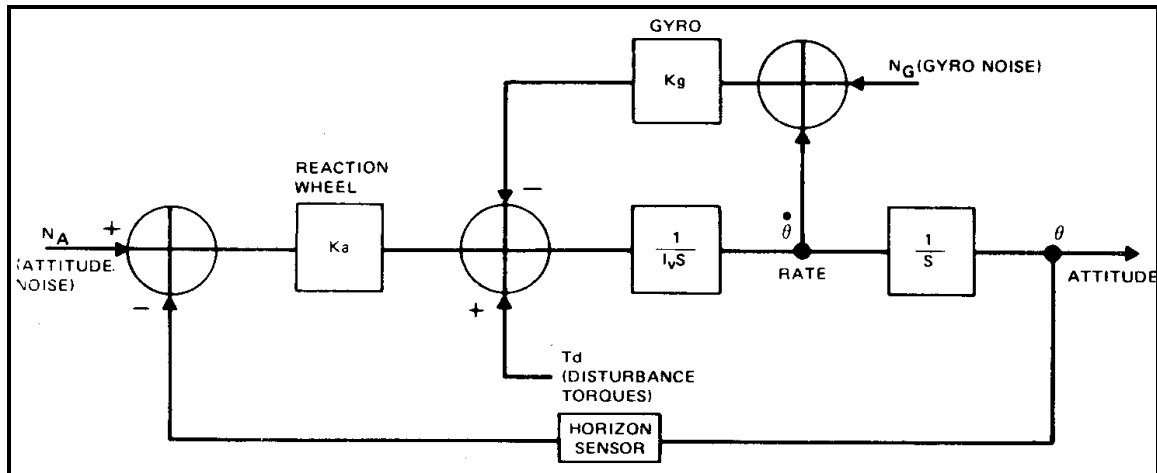
because the solution to (8) with the dynamics (1) is given by  $\underline{u} = K' \hat{\underline{x}}$  where K' is not the same as the K in (6) and  $\hat{\underline{x}}$  is the optimal estimate of  $\underline{x}$  obtained from the Kalman filter estimate of the state  $\underline{x}$ . In the implementation we are proposing here, the control does not correspond to the performance index (8) at all - in fact there is no performance index like (8) that gives the same control as was derived in (6). This is partly because of the pseudo inverse used in deriving the optimal gain in (6) (i.e. the  $(B^T B)^{-1} B^T$  term) and partly because any attempt to leave out the control weight R in (8) leads to infinite control gains (in order to make (8) correspond to a minimization of P, the covariance matrix, requires that R be zero).

Because the introduction of a filter into the control loop of an optimal system destroys the gain and phase margins that the optimal design has (infinite gain margin and at least 60° of phase margin) it is clearly more desirable to utilize the optimal stochastic control gains given by (6). In so doing, a comsat controller that leaves structural dynamics out of the design will have the property that the added phase lags introduced by structural frequencies close to or within the control band will not cause loss of stability. The next section gives an example of a design using this approach.

## **AN EXAMPLE OF OPTIMAL STOCHASTIC CONTROLLER FOR A COMMUNICATION SATELLITE**

The control system considered for a typical comsat uses three axes stabilization with three orthogonal reaction wheels. The attitude is measured using a horizon sensor and the angular rates sensed by three orthogonal rate gyros. A magnetic coil around the solar array is used to eliminate solar pressure torques and jets are incorporated for station keeping.

The control configuration is shown in Fig. 1 (a single axis); it uses full state feedback (position and rate) with the feedback gains chosen so as to minimize the rms angular rate and attitude. This is a classical approach to the problem formulated above when we are minimizing both disturbance torque and sensor noise effects while maintaining gain and phase margin that makes the design insensitive to parameter variations.



Since in its basic mode of operation the geostationary communication satellite requires no rapid slewing maneuvers and associated settling time requirements, the control problem is one of maintaining the attitude against very low frequency disturbances, such as solar, gravity gradient, magnetic and thermal torques, as well as the noises introduced by the horizon sensors and gyros. To compute these disturbances we use the transfer functions between the vehicle rate and the disturbances and sensor noises given by

$$\dot{\Theta}(s) = \frac{2\zeta s N_G(s) + s N_A(s) \omega_c}{\omega_c \left( \frac{s^2}{\omega_c^2} + \frac{2\zeta s}{\omega_c} + 1 \right)} \quad (9)$$

$$\dot{\Theta}(s) = \frac{T_d(s) s / (I_v \omega_c^2)}{\left( \frac{s^2}{\omega_c^2} + \frac{2\zeta s}{\omega_c} + 1 \right)} \quad (10)$$

where  $\omega_c^2 = K_a / I_v$  and  $K_g = 2\zeta / \omega_c$

Using an assumed white noise characteristic for the attitude  $N_A$  and gyro noise  $N_G$  in (9), the resulting satellite stability, on a one-sigma basis is given by

$$\sigma_{\theta} = \left\{ N_G^2 \zeta \omega_c + \frac{N_A^2 \omega_c^3}{4\zeta} \right\}^{1/2} \quad (11)$$

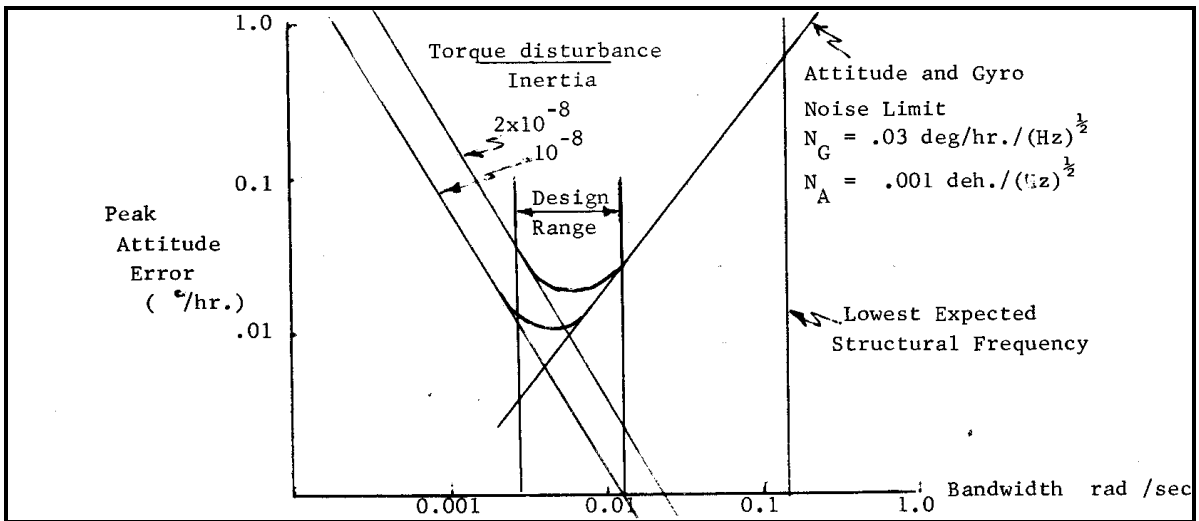
From Eq. (10), the satellite peak LOS rate levels resulting from cyclic torque disturbances (orbital rate) becomes

$$\dot{\theta}_{\max} = \frac{T_{d \max} \omega_o}{I_v \omega_c} \quad (12)$$

The LOS attitude and rate errors are plotted in Fig. 2 as a function of the control system bandpass ( $\omega_c$ ) for given attitude and gyro noise levels, and different torque disturbances to vehicle inertia ratios ( $T_{d \max} / I_v$ ). Note that as the bandpass  $\omega_c$  increases, the peak LOS errors due to torque disturbance decreases while the errors due to gyro and attitude sensor noise increases. Using the nominal gyro noise level and the attitude noise and disturbance torque to inertia ratio results in an optimum closed loop bandpass range of 0.004 to 0.04 rad/sec. Also shown on the figure is a lower limit on bandpass of 0.314 rad/sec (0.05 Hz) to prevent interaction of the control loop dynamics with any structural modes.

The net result of this simplified conceptual design is a specification for the bandpass of the control loop of 0.04 rad/sec. This results in a 0.20 deg/hr peak rate stability error and 0.008 deg peak attitude error. This conceptual design considers only a single axis. We extended the design to include all three axes with a magnetic unloading loop. Also included in this analysis is the solar array dynamics, the sloshing of the RCS propellant, and the solar, magnetic, and gravity gradient disturbances. To determine how large the solar array can be before control performance is degraded, a simulation was used that, contained all of the nonlinear actuator and sensor characteristics.

The primary torque disturbance acting on the satellite is due to solar pressure on an assumed 600 ft<sup>2</sup> solar array area with a large imbalance moment arm of approximately 0.1 ft. The resulting torque disturbance ( $1 \times 10^{-4}$  ft-lb) is cyclic at orbital rate acting about the X (roll) and Z (yaw) axes out of phase by 90 deg. This cyclic torque results in every increasing cyclic momentum storage requirement which must be unloaded over the 9-year mission period. An air core magnetic unloading system has been identified as a baseline approach for this application. Magnetic unloading can have a significant effect, however, on stability of the spacecraft because of undesirable cross coupling between the coil's magnetic dipole and the earth's field which cannot be compensated for during any given part of one orbit. Over a long period, however, (one orbit or more) the average reaction



( 0 ) 6 x 12

$$A = \begin{bmatrix} 0 & 1 & 0 & 0 & \omega_0 & 0 & 0 & 0 & 0 & 0 & 0 & 0 \\ H_{01} & -2\omega_0 \dot{\omega} & -2\omega_0 \ddot{\omega} & -2\dot{\omega} \omega_0 & 0 & -\frac{H_{03}}{I_{xx}} & 0 & 0 & \frac{L_{11}}{I_{xx}} & \frac{L_{12}}{I_{xx}} & \frac{L_{13}}{I_{xx}} & \frac{L_{14}}{I_{xx}} \\ 0 & 0 & 0 & 1 & 0 & 0 & 0 & 0 & 0 & 0 & 0 & 0 \\ -\frac{3\omega_0^2 I_{yy}}{I_{yy}} & \frac{I_{yz} \omega_0}{I_{yy}} & \frac{H_{02}}{I_{yy}} & 0 & 0 & -\frac{I_{yz} \omega_0}{I_{yy}} & 0 & 0 & 0 & \frac{L_{21}}{I_{yy}} & \frac{L_{22}}{I_{yy}} & \frac{L_{23}}{I_{yy}} \\ \omega_0 & 0 & 0 & 0 & 0 & 1 & 0 & 0 & 0 & 0 & 0 & 0 \\ -\frac{3\omega_0^2 I_{zz}}{I_{zz}} & \frac{H_{04}}{I_{zz}} & \frac{3\omega_0^2 I_{yz}}{I_{zz}} & \frac{2I_{yz} \omega_0}{I_{zz}} & 0 & \frac{I_{yz} \omega_0}{I_{zz}} & -\frac{\omega_0}{I_{zz}} & 0 & 0 & \frac{L_{31}}{I_{zz}} & \frac{L_{32}}{I_{zz}} & \frac{L_{33}}{I_{zz}} \end{bmatrix}$$

WHERE:

$$H_{01} = 3\omega_0^2 (I_{zz} - I_{yy})$$

$$H_{02} = 3\omega_0^2 (I_{zz} - I_{xx})$$

$$H_{03} = \omega_0 (I_{zz} - I_{yy})$$

$$H_{04} = \omega_0 (I_{xx} - I_{yy})$$

$$L_{11} = -(B_y^2 + B_z^2)$$

$$L_{12} = -B_x B_y$$

$$L_{13} = B_x B_z$$

$$L_{21} = -(B_x^2 + B_z^2)$$

$$L_{22} = B_y B_z$$

$$L_{23} = B_x B_z$$

$$L_{31} = B_x B_z$$

$$L_{32} = B_y B_z$$

$$L_{33} = -(B_x^2 + B_y^2)$$

= B

$$I = \begin{bmatrix} 0 & 0 & 0 & 0 & 0 & 0 \\ I_{xx} & 0 & 0 & 0 & 0 & 0 \\ 0 & 0 & 0 & 0 & 0 & 0 \\ 0 & 0 & I_{yy} & 0 & 0 & 0 \\ 0 & 0 & 0 & 0 & 0 & 0 \\ 0 & 0 & 0 & I_{zz} & 0 & 0 \end{bmatrix}$$

I 6x6

DEFINITION OF TERMS:

$I_{xx}, I_{yy}, I_{zz}$  = MOMENTS OF INERTIA ABOUT X, Y, & Z BODY AXES

$I_{xz}, I_{yz}, I_{xy}$  = CROSS PRODUCTS OF INERTIA

$\omega_0$  = ORBITAL RATE

$B_x, B_y, B_z$  = EARTH'S FIELD VECTORS IN ORBITAL COORDINATES

$\phi, \theta, \psi$  ARE EULER ANGLES

$p, q$  AND  $r$  ARE BODY RATES

$h_{\omega_i}$  (i = 1, 2, 3) ARE WHEEL MOMENTA

$\delta_i$  (i = 1, 2, 3) ARE CURRENTS IN MAGNETIC LOOPS

wheel speeds will be kept within acceptable levels. Another problem which further

complicates this problem in geostationary orbit is the relatively low levels of the earth's field (< 120 gamma). This makes it extremely difficult to sense the level of this field in the presence of the solar array dipole and other ferro-magnetic equipment distributed throughout the vehicle. For these reasons a magnetometer is not part of the control configuration for the unloading system. The exclusion of a magnetometer would not be critical if the earth's field could be predicted accurately, as it can during quiet periods of the sun. It is during solar storms that the problem must be addressed. An analysis was therefore performed to determine the effect that solar quiet and storm periods have on the stability of the satellite.

A closed loop optimal control was developed that used reaction wheels and magnetic unloading as a combined controller set with a simplified quiet days earth's field model. This design minimized a cost function defined by (13) for a set of linear first-order differential equations given by Eqs. (14) and (15) (the A matrix and B matrix for this design are shown in Fig. 3). Notice that this design is a more detailed version of the conceptual design above in that it includes the magnetic control and all three axes coupled together.

$$J = \int_0^{\infty} \underline{x}^T Q \underline{x} + \underline{u}^T R \underline{u} dt \quad (13)$$

$$\underline{x} = A\underline{x} + B\underline{u} \quad (14)$$

$$\underline{u} = K\underline{x}$$

where:

$j$  = cost function which was selected to attempt to match the bandwidth specified.

$\underline{x}$  = state vector (12x1) - the first six states are the rigid body pos. and rate and the second six are the wheel speeds and mag. loop cur.

$\underline{u}$  = control vector (6x1)

$Q$  = weighting matrix on states (12x12)

$R$  = weighting matrix on controls (6x6)

$A, B$  = matrices which define system dynamics (Fig. 3)

$K$  = gain matrix for optimally controlling the satellite ( 6 x 12).

With the resulting optimal gain matrix ( $K$ ) obtained from this analysis, a covariance analysis was then performed to determine the variance on each of the system states ( $\underline{x}$ ) for a combined set of random disturbance levels on the system (solar torques) and measurement noises (attitude and gyro noise levels).



The resulting closed loop characteristics and one sigma variances on the system parameters are presented in Fig. 4. Significant points to be made about these results are:

- Reaction wheel closed loop bandpass is below 0.05 rad/sec as identified in the conceptual design above
- Combined LOS (pitch, roll, yaw ) RSS error does not exceed 0.015 deg ( $3\sigma$ ) well below the 0.10 deg allowable
- Wheel momentum storage levels can be held to below 3 ft-lb-sec ( $1\sigma$ ) on an indefinite basis. This value compares favorably with the 15 ft-lb-sec storage capacity that would be required after two orbits if no magnetic unloading was provided.

Our preliminary analysis included the solar array modes for a two wing array configuration. This array had an estimated first mode frequency of 0.25 Hz. To verify the frequencies estimated by simplified preloaded string and beam analysis, the array was modelled in NASTRAN (Fig. 5). Central mast stiffness and mass and blanket mass data were obtained from the manufacture specification for the solar array. With a 20 lb preload, modes were calculated and are summarized in Fig. 5). The lower modes are primarily due to blanket motion rather than beam bending. Frequencies are lower than those predicted by pretensioned string theory due to edge flapping of the blanket.

Figure 6 represents a three-axis time history digital simulation run that demonstrates the ability of the attitude control design to hold the accuracies required over an orbit. The simulation included effects such as reaction wheel friction, gyro and attitude noise, solar disturbance torques, magnetic unloading, solar array structural bending and momentum cross coupling due to orbital rotation rate.

A three axis satellite simulation program called SATSIM was used in the final design verification. The time history of the attitudes and the momentum wheel angular momenta are shown in Fig. 6. Also shown is the disturbance torques that perturb the satellite over an orbit. The attitude traces clearly show the noises in the simulation, and the fact that the maximum rates are well below the required pointing rates and attitude requirements. To determine the effect of solar array modes that move into the control passband, the solar array size was altered in such a way that the first mode frequencies moved well within the control passband. The result of a simulation of this parameter variation showed that the control system remained stable with little or no performance degradation even when the modes were two orders of magnitude smaller in frequency. This result is a consequence of the collocation of the sensor and actuator set. From the point of view of classical control, such collocation means that the poles and zeros of the infinite number of structural modes

must alternate on the imaginary axis (when there is no damping). This alternation means that if full state feedback is used on the rigid body there is no way for the gains to cause the root locus to move into the right half plane. Thus the infinite gain margin property of the optimal design carries through when infinite flexible modes are added.

## CONCLUSION

In a study that we performed for NASA Marshall Space Flight Center (Ref.1), we showed that the problem of control of the flexible motion of a large space structure, whose dimensions were on the order of 100 meters, is possible. This result may be easily applied to communication satellites of the size that would be expected in the 1990's. The key conclusion of that study, as well as of this, is that the control problem is best handled by measuring as many states as possible and by using "full state feedback" from each of the measurements. In this study we have shown that such a design approach yield significant dividends in the "robustness" of the resulting design (i.e. gain and phase margins). In the MSFC study we also concluded that such an approach gives reasonable insensitivity to structural dynamics parameters even when sensors are dispersed about the structure (in that study, 52 strain gages were used to determine the motions at 52 dispersed points on the structure). As part of the presentation accompanying this paper, a movie of the MSFC structure was shown. This movie shows both discrete and continuous control systems designed for that study.

## References

1. Gran, R., Rossi, M. and Moyer H. "Optimal Digital Control of Large Space Structures" AAS Journal April 1979 .

Fig.4 Results of Covariance Analysis and Closed Loop Poles

---

Pole Locations    - Reaction Wheel Loops -0.093,-0.091,-0.04,-0.037,-0.043± 0.043j  
                           - Magnetic Unloading Loops -0.00023 ± 0.000245j and -0.00011

---

### Uncertainty in Various States (rms)

State	Roll	Pitch	Yaw
Attitude (deg.)	0.0004	0.001	0.0055
Attitude Rate Deg./Hr.	0.09	0.08	0.110
Wheel Momentum Ft.Lb.Sec.	2.4	0.9	3.0

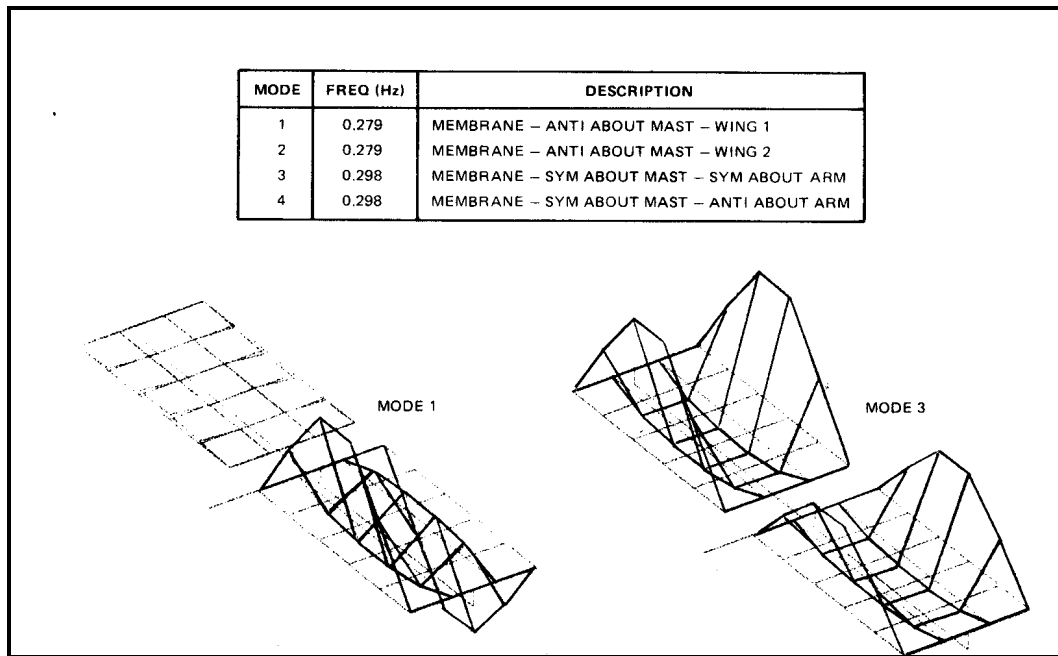


Fig. 5 Results of NASTRAN Analysis of Solar Array and the First Four Modes  
 These modes, mode shapes and mode masses were used in the SATSIM

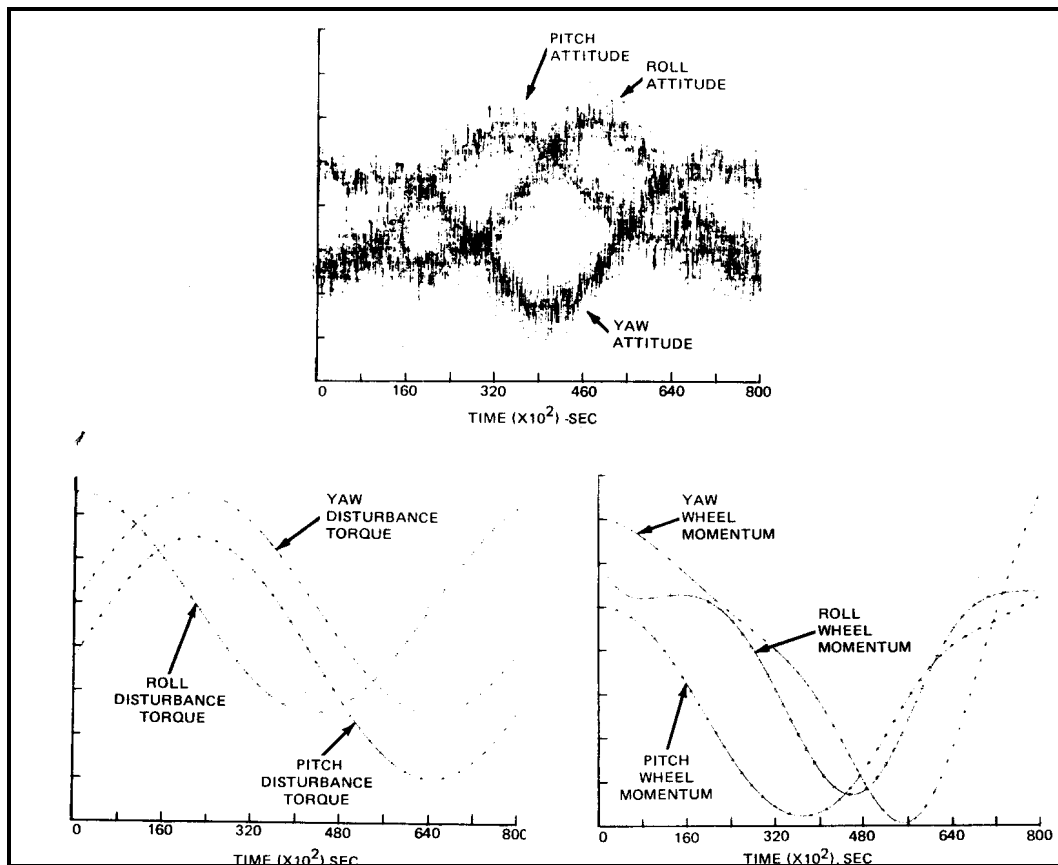


Fig. 6 Results of Satellite Simulation (SATSIM) for the Comsat Design